ACS Medicinal Chemistry Letters

Letter

Cite This: ACS Med. Chem. Lett. XXXX, XXX, XXX−XXX

Discovery of Orally Bioavailable Selective Inhibitors of the Sodium-Phosphate Cotransporter NaPi2a (SLC34A1)

Kevin J. Filipski,*[,†] Matthew F. Sammons,[†] Samit K. Bhattacharya,[†] Jane Panteleev,[‡,∥] Janice A. Brown,[‡] Paula M. Loria,[‡] Markus Boehm,[†] Aaron C. Smith,[‡] Andre Shavnya,[‡] Edward L. Conn,[‡] Kun Song,[†,⊥] Yan Weng,[†] Carie Facemire,[†,#] Harald Jüppner,[§] and Valerie Clerin[†]

[†]Pfizer Worldwide Research & Development, 1 Portland Street, Cambridge, Massachusetts 02139, United States

[‡]Pfizer Worldwide Research & Development, 558 Eastern Point Road, Groton, Connecticut 06340, United States

[§]Endocrine Unit and Pediatric Nephrology Unit, Thier 10, Massachusetts General Hospital and Harvard Medical School, 50 Blossom Street, Boston, Massachusetts 02114, United States

Supporting Information

ABSTRACT: Sodium-phosphate cotransporter 2a, or NaPi2a (SLC34A1), is a solute-carrier (SLC) transporter located in the kidney proximal tubule that reabsorbs glomerular-filtered phosphate. Inhibition of NaPi2a may enhance urinary phosphate excretion and correct maladaptive mineral and hormonal derangements associated with increased cardiovascular risk in chronic kidney disease−mineral and bone disorder (CKD-MBD). To date, only nonselective NaPi inhibitors have been described. Herein, we detail the discovery of the first series of selective NaPi2a inhibitors, resulting from optimization of a high-throughput screening hit. The oral PK profile of inhibitor PF-06869206 (**6f**) in rodents allows for the exploration of the pharmacology of selective NaPi2a inhibition.

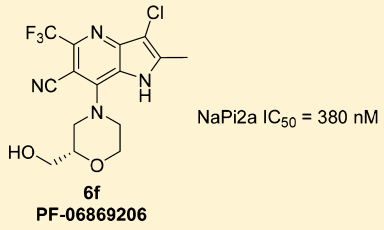

6f
PF-06869206

KEYWORDS: *SLC34A1, NaPi2a, sodium-phosphate cotransporter, kidney, proximal tubule, SLC*

Phosphate is an essential mineral component of bone, membranes, nucleic acids, nucleotides, and second messengers and is key to cellular processes involving kinases and phosphatases.[1,2] As such, a complex multiorgan regulatory interplay exists to maintain inorganic phosphate (Pi) homeostasis. Intestinal absorption of dietary Pi and urinary excretion control the flux of Pi into and out of the body, respectively, while bone is used as a reservoir in the regulation of Pi blood levels.

The three members of the NaPi2 family of solute carrier (SLC) sodium-phosphate cotransporters play a key role in phosphate homeostasis. NaPi2a (SLC34A1) and NaPi2c (SLC34A3) are located on the apical membrane of the kidney proximal tubule and function to reabsorb glomerular-filtered Pi.[3] NaPi2b (SLC34A2) is present on the apical membrane of the small intestine where it absorbs a portion of dietary Pi. The bone-derived hormone fibroblast growth factor 23 (FGF23) and parathyroid-derived parathyroid hormone (PTH) down-regulate NaPi2a and NaPi2c to increase urinary Pi excretion, while $1,25(OH)_2$-vitamin D_3 increases intestinal absorption of Pi by upregulating NaPi2b.[4,5]

Chronic kidney disease−mineral and bone disorder (CKD-MBD) is characterized by reduced glomerular filtration rate (GFR), altered calcium and Pi homeostasis, deranged levels of their regulatory hormones PTH, FGF23, and $1,25(OH)_2$-vitamin D_3, and compromised bone health.[6−8] Multiple lines of evidence indicate that elevated serum Pi and FGF23 excess directly and independently contribute to increased risk for cardiovascular mortality and morbidity in patients with CKD-MBD.[9−11] While oral Pi binders are used to manage sustained hyperphosphatemia in end stage renal disease, their use has not been recommended in earlier stages of the disease, and recent studies revealed no major improvement in Pi homeostasis.[8,12,13] Therefore, we pursued the development of a NaPi2a inhibitor as a novel approach to promote renal Pi excretion, reduce Pi and FGF23 overload, and decrease cardiovascular risk in predialysis CKD-MBD patients.[14−16]

To date, only nonselective NaPi2 inhibitors such as **1** and **2** (Figure 1) or NaPi2b inhibitors have been disclosed.[17−21] Selective inhibition of NaPi2a over NaPi2b will avoid the risk of pulmonary alveolar microlithiasis, a lung calcification disease associated with human NaPi2b mutations,[22−24] or limited efficacy in part caused by a compensatory upregulation of kidney Pi reabsorption associated with NaPi2b inhibition.[22,25] Furthermore, NaPi2a inhibitors are envisioned to be systemically available, unlike some intestinally restricted NaPi2b agents, and could offer straightforward pharmacokinetic monitoring.

In order to find chemical leads, a high-throughput screen (HTS) was performed by measuring the uptake of ^{33}P-radiolabeled Pi into HEK293 cells stably expressing NaPi2a.[26] The parental HEK293 cell line was shown to endogenously express another sodium-phosphate cotransporter, PiT-1 (SLC20A1)[28] (Figures S1 and S2) and, as such, showed a

Received: January 10, 2018
Accepted: April 4, 2018

DOI: 10.1021/acsmedchemlett.8b00013
ACS Med. Chem. Lett. XXXX, XXX, XXX−XXX

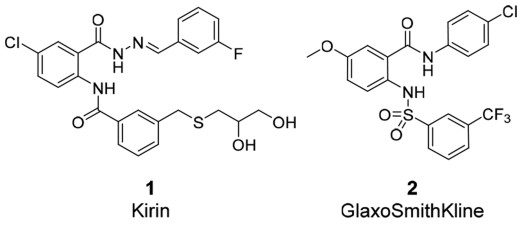

Figure 1. Representative nonselective literature NaPi2 inhibitors.

measurable, albeit lower, basal uptake of Pi. A series of related cell lines were also developed to probe the selectivity of analogues against other sodium-phosphate cotransporters: NaPi2b, NaPi2c, PiT-1, and PiT-2 (SLC20A2). Furthermore, cell lines containing the rat and mouse isoforms of NaPi2a and NaPi2c were developed. Compounds were also evaluated in a competition binding assay using membranes from NaPi2a-transfected cells (vide infra).

From the NaPi2a HTS of ~225,000 compounds in the Pfizer collection, **3a** was found as a hit and was profiled further (Table 1). Compound **3a** showed micromolar (IC_{50} = 6.5 μM) activity against NaPi2a and poor ligand and lipophilic efficiencies[29] (LE = 0.26, LipE = 1.2). However, in contrast to reference compounds **1** and **2**, hit **3a** showed some, albeit modest, selectivity against the other NaPi2 and PiT transporters as well as the parental cell line. Hit **3a** is very lipophilic (log*D* = 4.3, shake-flask method) and not surprisingly has poor apparent aqueous solubility measured at pH 6.5 (2 μM), very high human and rat liver microsome (HLM, RLM) clearance (HLM = 240 μL/min/mg; RLM > 560 μL/min/mg), and poor permeability as measured in RRCK cells.[27]

Scheme 1. Synthesis of Azaindole Analogues[a]

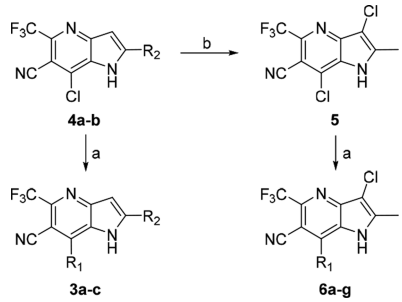

[a]Reagents and conditions: (a) amine, *i*-Pr_2NEt, CH_3CN, 80 °C or amine, *i*-Pr_2NEt, CsF, CH_3CN, 120 °C; (b) NCS, DMF, 20−30 °C.

The synthesis of derivatives of **3a** was performed as follows (Scheme 1). A literature method was used to synthesize compounds **4a−b**.[30] Standard S_NAr chemistry was used to install a 7-amino group on the azaindole core, leading to compounds **3a−c**. Alternatively, chlorination of the azaindole at the 3-position was effected with *N*-chlorosuccinimide to

Table 1. SAR around Azaindole Core and Literature Comparators

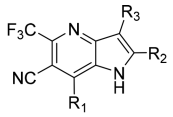

			IC_{50} (μM)[a]										
R_1	R_2	R_3	NaPi2a	NaPi2b	NaPi2c	PiT-1	PiT-2	Parental HEK	NaPi2a Binding K_i (μM)[a]	log*D*	RLM $Cl_{int,app}$ (μL/min/mg)	P_{app}[b] (10^{-6} cm/s)	Sol[c] (μM)
1	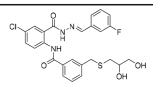		0.46 ± 0.019	0.15 ± 0.019	1.9 ± 0.051	5.4 ± 0.41	>27 ± 2.3	4.3 ± 0.21	0.69 ± 0.28	3.9	>560	<2.2	1.1
2	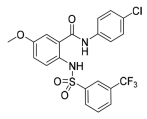		>7.3 ± 0.96	>3.3 ± 1.5	>7.5 ± 0.82	1.5 ± 0.52	6.2 ± 0.77	1.3 ± 0.30	>25	4.2	410	1.4	4.6
3a	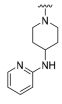	Me	H	6.5 ± 1.3	>19 ± 2.2	21 ± 2.6	>14 ± 3.2	>24 ± 0.38	>16 ± 3.0	14 ± 1.9	4.3	>560	2.8	2.0
3b	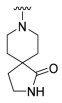	Me	H	1.5 ± 1.0	>25	>25	>25	>25	>25	2.0 ± 0.85	2.6	97	17	1.8
3c	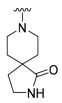	H	H	>15 ± 3.1	>25	>25	>25	>25	>25	10 ± 1.8	2.3	26	14	1.6
6a	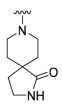	Me	Cl	0.10 ± 0.052	>25	>25	>25	>25	>25	0.082 ± 0.013	3.2	>560	25	1.9

[a]IC_{50}'s and K_i's are reported as the geometric mean of $n \geq 3$ ± standard error of the mean, except where otherwise noted. [b]Passive permeability (P_{app}) from the apical to basolateral (AB) direction was measured in Ralph Russ Canine Kidney (RRCK) cells as previously described.[27] [c]Aqueous solubility at pH 6.5.

DOI: 10.1021/acsmedchemlett.8b00013
ACS Med. Chem. Lett. XXXX, XXX, XXX−XXX

Table 2. SAR around 7-Position of Core

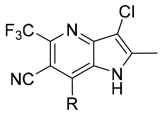

R	IC$_{50}$ (μM)[a] NaPi2a	NaPi2b	NaPi2c	PiT-1	PiT-2	Parental HEK	NaPi2a Binding K_i (μM)[a]	log*D*	RLM Cl$_{int,app}$ (μL/min/mg)	P$_{app}$ (10^{-6} cm/s)[d]	Sol (μM)[e]
6b	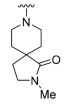	0.12 ± 0.014	>60	>60	>60	>26 ± 4.3	>60	0.53 ± 0.22	3.0	>560	11	56
6c	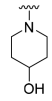	0.13 ± 0.032	>25	>25	>25	>25	>25	0.44 ± 0.11	3.3	NT[f]	10	2.6
6d		2.5 ± 0.42	>25	>25	>25	>25	>25	2.3 ± 0.34	1.0	<14	0.70	230
6e	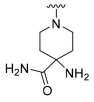	0.29 ± 0.048	>25	>25	>25	>25	>25	0.25 ± 0.11	2.1	16	5.0	4.2
6f		0.38 ± 0.032	>25	>25	>24 ± 0.81	>25	>25	0.75 ± 0.070	2.6	<14	15	46
6g		0.39 ± 0.038	>24[b]	>25	>24[b]	>24[c]	>24[c]	1.3[b]	2.4	<14	<11	54

[a]IC$_{50}$'s and K_i's are reported as the geometric mean of $n \geq 3$ ± standard error of the mean, except where otherwise noted. [b]$n = 1$. [c]$n = 2$. [d]Passive permeability (P$_{app}$) from the apical to basolateral (AB) direction was measured in Ralph Russ Canine Kidney (RRCK) cells as previously described.[27] [e]Aqueous solubility at pH 6.5. [f]NT = not tested.

Table 3. Rodent Potency of 6f

IC$_{50}$ (μM)[a] rat NaPi2a	rat NaPi2c	mouse NaPi2a	mouse NaPi2c
0.40 ± 0.047	>25	0.54 ± 0.099	>25

[a]IC$_{50}$'s are reported as the geometric mean of $n \geq 3$ ± standard error of the mean.

Scheme 2. Synthesis of Azaindole Analogue 6f[a]

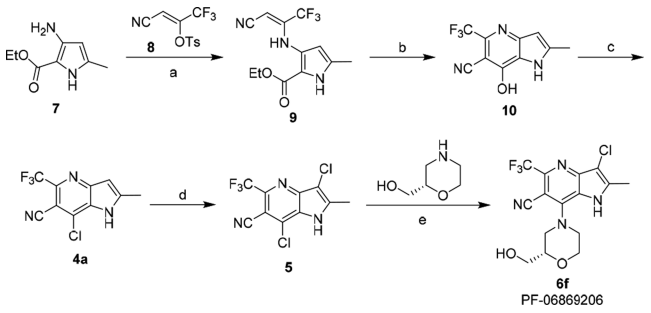

[a]Reagents and conditions: (a) *i*-Pr$_2$NEt, CH$_3$CN, −10 to −5 °C, 87%; (b) DBU, CH$_3$CN, 90 °C, 70%; (c) POCl$_3$, CH$_3$CN, 60 °C, 90%; (d) NCS, DMF, 30 °C, 76%; (e) *i*-Pr$_2$NEt, CH$_3$CN, 80 °C, 86%.

provide intermediate **5**, and analogous S$_N$Ar chemistry led to compounds **6a**–**g**.

In order to turn the initial hit **3a** into a useful tool to probe the pharmacology of selective NaPi2a inhibition, the 7-position of the azaindole core was first modified. Replacement of the piperidine 4-substituent with a spirocyclic lactam provided **3b**. This change resulted in increased LipE (3.6 vs 1.2) and significantly improved selectivity for inhibition of NaPi2a over the other sodium-phosphate cotransporters tested (all other IC$_{50}$'s > 25 μM, Figure S3). We also observed that the maximum inhibitory effect of **3b** in the NaPi2a-transfected cells was ∼75% of total Pi uptake (Figure S4). Since the HEK293 cell line endogenously expresses PiT-1, and the nonselective **1** (25 μM) was used to define 100% inhibition, our interpretation is that, after NaPi2a-transfection, the cells contain a ≤3:1 functional ratio of NaPi2a/PiT-1. This E_{max} attribute was maintained with future potent analogues from this series.

The SAR of the 2- and 3-positions of the azaindole core was examined next. Deletion of the 2-methyl group (**3c**) led to a significant loss of potency and LipE (<2.8), suggesting a beneficial lipophilic interaction in this location. The addition of a 3-chloro substituent (**6a**) yielded a 100 nM inhibitor with improved LipE (4.0), permeability, and excellent selectivity. However, the RLM clearance and aqueous solubility of **6a** were still very poor. Subsequent work to improve the ADME properties was done while maintaining the potent 3-chloro-2-methylazaindole core (Table 2).

The *N*-methylated lactam (**6b**) showed similar potency to **6a**; however, this did lead to a useful radioligand. The tritiated (C[^{3}H]$_3$) version of **6b** showed saturable binding to membranes from the NaPi2a-transfected cells with a K_d = 320 nM (Figures S5 and S6). This differs from parental cell

DOI: 10.1021/acsmedchemlett.8b00013
ACS Med. Chem. Lett. XXXX, XXX, XXX−XXX

Table 4. Rat and Mouse PK of 6f[a]

species	route	dose (mg/kg)	Cl (mL/min/kg)	V_{dss} (L/kg)	$t_{1/2}$ (h)	C_{max} (ng/mL)	t_{max} (h)	AUC_{0-24h} (ng·h/mL)	F (%)
Wistar−Han rat	IV	1[b]	15	3.1	4.8			1100	
Wistar−Han rat	PO	5[c]				720	0.75	4800	87
Wistar−Han rat	PO	50[c]				6000	1.0	77,000	140
C57BL6 mouse	IV	1[b]	22	0.86	0.75			760	
C57BL6 mouse	PO	5[c]				540	0.38	1000	27
C57BL6 mouse	PO	50[c]				11,000	1.5	92,000	240

[a]All values are the arithmetic mean of data from $n = 2$ animals. Rat plasma protein binding fraction unbound (PPB FU) = 0.0243; mouse PPB FU = 0.0287. [b]Vehicle: 10% DMSO/30% PEG-400/60% water (2 mL/kg). [c]Vehicle: suspension in 0.5% methylcellulose (10 mL/kg).

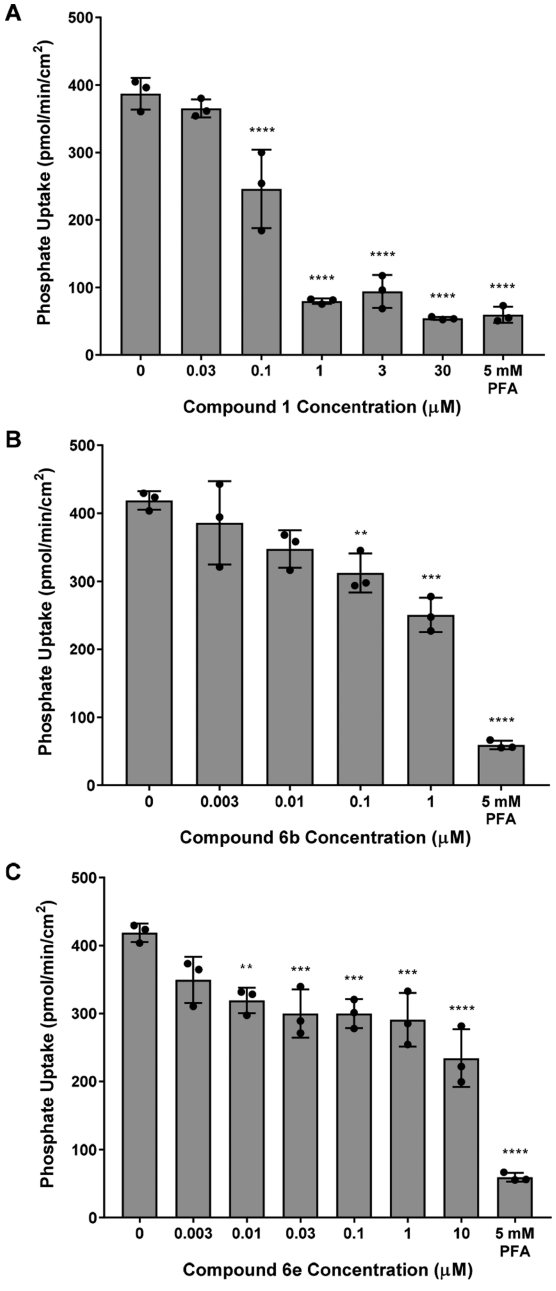

Figure 2. Inhibition of phosphate uptake in human proximal tubule cells by (A) **1**, (B) **6b**, and (C) **6e** compared with PFA. All three experiments from one donor. *$p \leq 0.05$, **$p \leq 0.01$, ***$p \leq 0.001$, ****$p \leq 0.0001$; one-way ANOVA with Dunnett's comparison to 0 μM control.

membranes where saturable binding was not observed. This radioligand was used to develop a competition binding assay where the ability of test compounds to displace tritiated **6b** was measured. K_i's shown in Tables 1 and 2 exhibit good agreement between the functional and binding potencies. Although the radioligand is competitive with nonselective **1**, the structural reasoning behind this difference remains unknown. Furthermore, the new inhibitors are functionally selective; it is unknown if they bind to the other phosphate transporters beyond the parental cells.

Through further SAR efforts, the presence of a hydrogen-bond acceptor (HBA) near the 3- or 4-position of the piperidine proved key to obtaining good potency. This can be observed with 4-hydroxypiperidine with one of the highest ligand efficiencies (LE = 0.41) observed for the entire series. This compound still had poor solubility, so we pursued multiple approaches to improve this property. By adding a charged center as in the primary amine **6d** (pK_a = 8.9), solubility was greatly improved (230 μM), unfortunately at the cost of potency (2.5 μM). The amino amide **6e** improved potency, further confirming our HBA hypothesis, but since this is a much weaker base (pK_a = 5.7), the solubility at pH 6.5 was greatly reduced. An alternative strategy of increasing flexibility in an effort to break efficient crystal packing interactions led to **6f** (PF-06869206). Morpholino-methanol **6f** showed a balance of attributes with 380 nM NaPi2a inhibition potency, excellent subtype selectivity, and acceptable aqueous solubility (46 μM). Furthermore, permeability is good (14×10^{-6} cm/s), and RLM clearance is low (<14 μL/min/mg; HLM = 39 μL/min/mg). The enantiomer, **6g**, was also synthesized and has similar potency.

Compound **6f** was further profiled for potency in the rodent NaPi2a and NaPi2c cell lines (Table 3). This analogue showed comparable submicromolar activity for the human, rat, and mouse NaPi2a isoforms and was selective over rodent NaPi2c.

To support chronic in vivo studies, a large-scale synthesis of **6f** was developed (Scheme 2). Pyrrole **7**[31] was reacted with enol tosylate **8**[32] to form **9**. DBU was used to effect pyridine ring cyclization to give azaindole **10**. Conversion of 7-hydroxyazindole **10** to the corresponding 7-chloroazaindole **4a** was accomplished using phosphorus oxychloride. *N*-Chlorosuccinimide chlorination of the 3-position yielded **5** and S_NAr with (*S*)-morpholin-2-ylmethanol provided the desired **6f**.

Compound **6f** was evaluated in rodent PK studies to determine suitability for in vivo pharmacology exploration. Results showed moderate clearance in both rat and mouse (Table 4, Figure S7). Oral bioavailability at 5 mg/kg was good in rat and moderate in mouse. At higher oral doses of 50 mg/kg, supraproportional increases in exposure were observed in both species, suggestive of saturation of clearance.

DOI: 10.1021/acsmedchemlett.8b00013
ACS Med. Chem. Lett. XXXX, XXX, XXX−XXX

The ability of two selective NaPi2a inhibitors from this newly identified series, **6b** and **6e**, to inhibit Pi uptake in human proximal tubule cells was characterized in vitro. As determined by qPCR, these cells retained expression of NaPi2a, NaPi2c, PiT-1, and PiT-2 (Figure S8). Nonselective inhibitor phosphonoformic acid (PFA)[3,28] at 5 mM inhibited on average 84% of Pi uptake and was used as a positive control across experiments (Figures 2 and S9). At a common test concentration of 1 μM and using cells from three different donors, nonselective inhibitor **1** and selective NaPi2a inhibitors **6b** and **6e** showed mean Pi inhibition values of 79, 41, and 32%, respectively. All three inhibitors displayed concentration-dependent inhibition of Pi uptake. These results confirm the selectivity profile of the newly identified series in a highly relevant in vitro functional assay and indicate that NaPi2a plays a significant role in human proximal tubule Pi reabsorption.

In summary, PF-06869206 (**6f**) is the first orally bioavailable selective NaPi2a inhibitor and, as such, represents a pharmacological tool to probe the functional effects of selective NaPi2a inhibition in vivo. Results of these efforts will be communicated in a future disclosure.

■ ASSOCIATED CONTENT

Supporting Information

The Supporting Information is available free of charge on the ACS Publications website at DOI: 10.1021/acsmedchemlett.8b00013.

Synthetic procedures along with cell line expression, binding studies, and cellular phosphate uptake assays (PDF)

■ AUTHOR INFORMATION

Corresponding Author

*E-mail: kevin.filipski@pfizer.com.

ORCID

Kevin J. Filipski: 0000-0003-0845-5723
Matthew F. Sammons: 0000-0001-6472-0646
Markus Boehm: 0000-0002-7025-3287
Aaron C. Smith: 0000-0001-6796-5155

Present Addresses

[‖](J.P.) Amgen Inc., 360 Binney Street, Cambridge, Massachusetts 02141, United States.
[⊥](K.S.) IMED Oncology, AstraZeneca Pharmaceuticals, Waltham, Massachusetts 02451, United States.
[#](C.F.) EBSCO Health, 10 Estes Street, Ipswich, Massachusetts 01938, United States.

Author Contributions

The manuscript was written through contributions of all authors. All authors have given approval to the final version of the manuscript.

Notes

(1) All procedures on animals were in accordance with regulations and established guidelines and were reviewed and approved by Pfizer's Institutional Animal Care and Use Committee. (2) Research was conducted on human tissue acquired from a third party that has been verified as compliant with Pfizer policies, including IRB/IEC approval. (3) Compound **6f** (PF-06869206) has been made commercially available via MilliporeSigma (catalog # PZ0389).
The authors declare no competing financial interest.

■ ACKNOWLEDGMENTS

The authors wish to thank Professor Colin D. A. Brown, Git Chung, Karen Atkinson, Jeffrey Chabot, Brian Chekal, Steven B. Coffey, Kentaro Futatsugi, Daniel W. Kung, Chia-Chin (Wilson) Lee, John Litchfield, Suman Luthra, Kim McClure, Klaas Schildknegt, and WuXi AppTec. H.J. is supported by NIH grants DK11794 and DK46718.

■ ABBREVIATIONS

Pi, inorganic phosphate; NaPi2a, sodium-phosphate transporter 2a; SLC34A1, solute carrier transporter 34A1; FGF23, fibroblast growth factor-23; PTH, parathyroid hormone; CKD-MBD, chronic kidney disease−mineral and bone disorder; GFR, glomerular filtration rate; HTS, high throughput screen; LipE, lipophilic efficiency; RLM, rat liver microsome; RRCK, Ralph Russ Canine Kidney; ADME, absorption, distribution, metabolism, and excretion; LE, ligand efficiency; HBA, hydrogen bond acceptor

■ REFERENCES

(1) Wagner, C. A.; Hernando, N.; Forster, I. C.; Biber, J. The SLC34 family of sodium-dependent phosphate transporters. *Pfluegers Arch.* **2014**, *466* (1), 139−153.
(2) Hruska, K. A.; Mathew, S.; Lund, R.; Qiu, P.; Pratt, R. Hyperphosphatemia of chronic kidney disease. *Kidney Int.* **2008**, *74* (2), 148−157.
(3) Forster, I. C.; Hernando, N.; Biber, J.; Murer, H. Phosphate transporters of the SLC20 and SLC34 families. *Mol. Aspects Med.* **2013**, *34* (2−3), 386−395.
(4) Andrukhova, O.; Zeitz, U.; Goetz, R.; Mohammadi, M.; Lanske, B.; Erben, R. G. FGF23 acts directly on renal proximal tubules to induce phosphaturia through activation of the ERK1/2-SGK1 signaling pathway. *Bone* **2012**, *51* (3), 621−628.
(5) Gattineni, J.; Friedman, P. A. Regulation of hormone-sensitive renal phosphate transport. *Vitam. Horm.* **2015**, *98*, 249−306.
(6) Block, G. A.; Ix, J. H.; Ketteler, M.; Martin, K. J.; Thadhani, R. I.; Tonelli, M.; Wolf, M.; Jüppner, H.; Hruska, K.; Wheeler, D. C. Phosphate homeostasis in CKD: report of a scientific symposium sponsored by the National Kidney Foundation. *Am. J. Kidney Dis.* **2013**, *62* (3), 457−73.
(7) Vervloet, M. G.; Sezer, S.; Massy, Z. A.; Johansson, L.; Cozzolino, M.; Fouque, D. & on behalf of the ERA−EDTA Working Group on Chronic Kidney Disease−Mineral and Bone Disorders and the European Renal Nutrition Working Group. The role of phosphate in kidney disease. *Nat. Rev. Nephrol.* **2017**, *13* (1), 27−38.
(8) Kidney Disease: Improving Global Outcomes (KDIGO) CKD-MBD Update Work Group. KDIGO 2017 clinical practice guideline update for the diagnosis, evaluation, prevention, and treatment of chronic kidney disease−mineral and bone disorder (CKD-MBD). *Kidney Int. Suppl.* **2017**, *7* (1), 1−59.
(9) Vo, T. M.; Disthabanchong, S. Are there ways to attenuate arterial calcification and improve cardiovascular outcomes in chronic kidney disease? *World J. Cardiol.* **2014**, *6* (5), 216−226.
(10) Scialla, J. J.; Wolf, M. Roles of phosphate and fibroblast growth factor 23 in cardiovascular disease. *Nat. Rev. Nephrol.* **2014**, *10* (5), 268−278.
(11) Jono, S.; McKee, M. D.; Murry, C. E.; Shioi, A.; Nishizawa, Y.; Mori, K.; Morii, H.; Giachelli, C. M. Phosphate regulation of vascular smooth muscle cell calcification. *Circ. Res.* **2000**, *87* (7), E10−7.
(12) Waheed, A. A.; Pedraza, F.; Lenz, O.; Isakova, T. Phosphate control in end-stage renal disease: barriers and opportunities. *Nephrol., Dial., Transplant.* **2013**, *28* (12), 2961−2968.
(13) Liabeuf, S.; Ryckelynck, J. P.; El Esper, N.; Urena, P.; Combe, C.; Dussol, B.; Fouque, D.; Vanhille, P.; Frimat, L.; Thervet, E.; Mentaverri, R.; Prie, D.; Choukroun, G. for the FRENCH Study collaborators. Randomized clinical trial of sevelamer carbonate on

DOI: 10.1021/acsmedchemlett.8b00013
ACS Med. Chem. Lett. XXXX, XXX, XXX−XXX

serum klotho and fibroblast growth factor 23 in CKD. *Clin. J. Am. Soc. Nephrol.* **2017**, *12*, 1930.
(14) Christov, M.; Jüppner, H. Dietary phosphate: the challenges of exploring its role in FGF23 regulation. *Kidney Int.* **2013**, *84* (4), 639−641.
(15) Ohnishi, M.; Nakatani, T.; Lanske, B.; Razzaque, M. S. In vivo genetic evidence for suppressing vascular and soft-tissue calcification through the reduction of serum phosphate levels, even in the presence of high serum calcium and 1,25-dihydroxyvitamin D levels. *Circ.: Cardiovasc. Genet.* **2009**, *2* (6), 583−590.
(16) Isakova, T.; Ix, J. H.; Sprague, S. M.; Raphael, K. L.; Fried, L.; Gassman, J. J.; Raj, D.; Cheung, A. K.; Kusek, J. W.; Flessner, M. F.; Wolf, M.; Block, G. A. Rationale and approaches to phosphate and fibroblast growth factor 23 reduction in CKD. *J. Am. Soc. Nephrol.* **2015**, *26* (10), 2328−2339.
(17) Edwards, R. M.; Franz, R. G.; Gaitanopoulos, D.; Weinstock, J. N-Aryl-2-sulfonamidobenzamides as phosphate transport inhibitors. WO2001005398, 2001.
(18) Weinstock, J. Inhibitors of sodium-dependent phosphate transport. *Expert Opin. Ther. Pat.* **2004**, *14* (1), 81−84.
(19) Eto, N.; Nagao, R.; Miyazaki, T. Preparation of benzamide compounds as phosphorus transport inhibitors. WO2004085382A1, 2004.
(20) Matsuo, A.; Negoro, T.; Seo, T.; Kitao, Y.; Shindo, M.; Segawa, H.; Miyamoto, K. Inhibitory effect of JTP-59557, a new triazole derivative, on intestinal phosphate transport in vitro and in vivo. *Eur. J. Pharmacol.* **2005**, *517* (1−2), 111−9.
(21) Lewis, J. G.; Jacobs, J. W.; Reich, N.; Leadbetter, M. R.; Bell, N.; Chang, H.-T.; Chen, T.; Navre, M.; Charmot, D.; Carreras, C.; Labonte, E. Benzamide compounds as inhibitors of phosphate transport and their preparation. WO2012054110, 2012.
(22) Sabbagh, Y.; O'Brien, S. P.; Song, W.; Boulanger, J. H.; Stockmann, A.; Arbeeny, C.; Schiavi, S. C. Intestinal Npt2b plays a major role in phosphate absorption and homeostasis. *J. Am. Soc. Nephrol.* **2009**, *20* (11), 2348−2358.
(23) Huqun; Izumi, S.; Miyazawa, H.; Ishii, K.; Uchiyama, B.; Ishida, T.; Tanaka, S.; Tazawa, R.; Fukuyama, S.; Tanaka, T.; Nagai, Y.; Yokote, A.; Takahashi, H.; Fukushima, T.; Kobayashi, K.; Chiba, H.; Nagata, M.; Sakamoto, S.; Nakata, K.; Takebayashi, Y.; Shimizu, Y.; Kaneko, K.; Shimizu, M.; Kanazawa, M.; Abe, S.; Inoue, Y.; Takenoshita, S.; Yoshimura, K.; Kudo, K.; Tachibana, T.; Nukiwa, T.; Hagiwara, K. Mutations in the SLC34A2 gene are associated with pulmonary alveolar microlithiasis. *Am. J. Respir. Crit. Care Med.* **2007**, *175* (3), 263−268.
(24) Corut, A.; Senyigit, A.; Ugur, S. A.; Altin, S.; Ozcelik, U.; Calisir, H.; Yildirim, Z.; Gocmen, A.; Tolun, A. Mutations in SLC34A2 cause pulmonary alveolar microlithiasis and are possibly associated with testicular microlithiasis. *Am. J. Hum. Genet.* **2006**, *79* (4), 650−656.
(25) Hernando, N.; Myakala, K.; Simona, F.; Knopfel, T.; Thomas, L.; Murer, H.; Wagner, C. A.; Biber, J. Intestinal depletion of NaPi-IIb/Slc34a2 in mice: renal and hormonal adaptation. *J. Bone Miner. Res.* **2015**, *30* (10), 1925−1937.
(26) Wu, H.; Mao, C.; Duenstl, G.; Su, W.; Qian, S. Assay development of inducible human renal phosphate transporter Npt2A (SLC34A1) in Flp-In-Trex-HEK293 cells. *Eur. J. Pharmacol.* **2013**, *721* (1−3), 332−340.
(27) Di, L.; Whitney-Pickett, C.; Umland, J. P.; Zhang, H.; Zhang, X.; Gebhard, D. F.; Lai, Y.; Federico, J. J., 3rd; Davidson, R. E.; Smith, R.; Reyner, E. L.; Lee, C.; Feng, B.; Rotter, C.; Varma, M. V.; Kempshall, S.; Fenner, K.; El-Kattan, A. F.; Liston, T. E.; Troutman, M. D. Development of a new permeability assay using low-efflux MDCKII cells. *J. Pharm. Sci.* **2011**, *100* (11), 4974−4985.
(28) Forster, I. C.; Hernando, N.; Biber, J.; Murer, H. Phosphate transport kinetics and structure-function relationships of SLC34 and SLC20 proteins. *Curr. Top. Membr.* **2012**, *70*, 313−356.
(29) Ryckmans, T.; Edwards, M. P.; Horne, V. A.; Correia, A. M.; Owen, D. R.; Thompson, L. R.; Tran, I.; Tutt, M. F.; Young, T. Rapid assessment of a novel series of selective CB(2) agonists using parallel synthesis protocols: A Lipophilic Efficiency (LipE) analysis. *Bioorg. Med. Chem. Lett.* **2009**, *19* (15), 4406−4409.
(30) Huard, K.; Ahn, K.; Amor, P.; Beebe, D. A.; Borzilleri, K. A.; Chrunyk, B. A.; Coffey, S. B.; Cong, Y.; Conn, E. L.; Culp, J. S.; Dowling, M. S.; Gorgoglione, M. F.; Gutierrez, J. A.; Knafels, J. D.; Lachapelle, E. A.; Pandit, J.; Parris, K. D.; Perez, S.; Pfefferkorn, J. A.; Price, D. A.; Raymer, B.; Ross, T. T.; Shavnya, A.; Smith, A. C.; Subashi, T. A.; Tesz, G. J.; Thuma, B. A.; Tu, M.; Weaver, J. D.; Weng, Y.; Withka, J. M.; Xing, G.; Magee, T. V. Discovery of fragment-derived small molecules for in vivo inhibition of ketohexokinase (KHK). *J. Med. Chem.* **2017**, *60* (18), 7835−7849.
(31) Gangjee, A.; Li, W.; Yang, J.; Kisliuk, R. L. Design, synthesis, and biological evaluation of classical and nonclassical 2-amino-4-oxo-5-substituted-6-methylpyrrolo[3,2-d]pyrimidines as dual thymidylate synthase and dihydrofolate reductase inhibitors. *J. Med. Chem.* **2008**, *51* (1), 68−76.
(32) Michelotti, E. L.; Springman, E. B.; Nguyen, D.; Shetty, R. S.; Lee, Y.; Moffett, K. K.; Ludington, J. L.; Fujimoto, T. T.; Konteatis, Z. D.; Liu, B.; Hollinger, F.; Dorsey, B. D. Preparation of heteroaryl-aryl ureas as inhibitors of protein kinases. WO2006062982, 2006.

DOI: 10.1021/acsmedchemlett.8b00013
ACS Med. Chem. Lett. XXXX, XXX, XXX−XXX